

## Microturbine and Thermoelectric Generator Combined System: A Case Study

Alvise Miozzo\*, Stefano Boldrini, Alberto Ferrario, and Monica Fabrizio

*Institute for Condensed Matter Chemistry and Technologies for Energy, National Research Council of Italy,  
Corso Stati Uniti 4, 35127 Padua, Italy*

Waste heat recovery is one of the suitable industrial applications of thermoelectrics. Thermoelectric generators (TEG) are used, commonly, only for low-mid size power generation systems. The low efficiency of thermoelectric modules generally does not encourage their combination with high power and temperature sources, such as gas turbines. Nevertheless, the particular features of thermoelectric technology (no moving parts, scalability, reliability, low maintenance costs) are attractive for many applications. In this work, the feasibility of the integration of a TE generator into a cogeneration system is evaluated. The cogeneration system consists of a microturbine and heat exchangers for the production of electrical and thermal energy. The aim is to improve electric power generation by using TE modules and the “free” thermal energy supplied by the cogeneration system, through the exhaust pipe of the microturbine. Three different solutions for waste heat recovery from the exhausts gas are evaluated, from the fluid dynamics and heat transfer point of view, to find out a suitable design strategy for a combined power generation system.

**Keywords:** Thermoelectric Generator, Waste Heat Recovery, Micro Gas Turbine, CFD Simulation.

### 1. INTRODUCTION

Thermoelectric materials are used to produce electrical power from heat flow across a temperature gradient. A module for power generation is an assembly of thermoelectric couples of *n*-type and *p*-type semiconductors connected electrically in series and thermally in parallel. The thermoelectric generator is realized by coupling the modules with a heat source (hot side) and a heat sink (cold side). The electrical power is generated with efficiency:

$$\eta = P/Q_h$$

where *P* [W] is the generated electrical power and *Q<sub>h</sub>* [W] the thermal flux entering the module.

The conversion efficiency can also be expressed as:<sup>1,2</sup>

$$\eta = \frac{\Delta T}{T_h} \frac{\sqrt{1 + Z_c \bar{T}} - 1}{\sqrt{1 + Z_c \bar{T}} + (T_c/T_h)}$$

where  $\Delta T = T_h - T_c$  is the temperature difference,  $\bar{T}$  is the average temperature,  $\Delta T/T_h$  is the Carnot efficiency and  $Z_c \bar{T}$  is the device figure of merit, with:

$$Z_c = \left[ \frac{\alpha_{pn}}{(\rho_p k_p)^{1/2} + (\rho_n k_n)^{1/2}} \right]^2$$

where  $\alpha_{pn} = \alpha_p - \alpha_n$  is the Seebeck coefficient [V/K] of the couple,  $\rho_p$  and  $\rho_n$  [Ωm] are the electrical resistivity values of the *p* and *n* type legs respectively, while  $k_p$  and  $k_n$  [Wm<sup>-1</sup>K<sup>-1</sup>] are the thermal conductivities. Thermoelectric technology has some highly valuable advantages: it does not require any moving part, it provides silent operations (no vibrations), high scalability and modularity. These features have encouraged the use of thermoelectric devices for aerospace and automotive applications. Nevertheless, currently available thermoelectric power modules present quite low efficiency (5 to 8%); state-of-the-art materials show  $ZT_{\text{average}} \sim 0.9$  at medium hot side temperature.<sup>3</sup> For these reasons, thermoelectrics can not compete with heat engine power generators for stand-alone systems, in terms of efficiency. In some industries, however, there is limited opportunity to reuse waste

\* Author to whom correspondence should be addressed.

thermal energy. This makes TE power generation attractive for waste heat recovery in industrial processes like aluminium melting, metal casting, cement kilns, etc.<sup>3,4</sup>

In this work, an application of thermoelectric generation at a medium temperature was evaluated. The issue is the feasibility of waste heat recovery from a micro gas turbine (MGT) for thermoelectric power generation. Waste heat from micro gas turbines can be reused for hot water production. Nevertheless, pressure drops in exhaust gas flow through the required gas/water heat exchanger may cause decrease in turbine efficiency.<sup>5</sup> Integrating a thermoelectric generator (TEG) into the cogeneration system consisting of power module (MGT) and heat exchanger enhances electric power generation. As minimum target, the amount of electric power to produce via thermoelectric generator has been fixed at 500 W. It is reasonable to expect that such an increment of generated power could compensate the potential efficiency decrease due to the flow of exhaust gas across a heat exchanger. Three suitable configurations for a coupled system micro gas turbine (MGT) and thermoelectric generator (TEG) to increase electrical power production have been evaluated. The theoretical framework for the evaluation of the performances of the coupled system is provided by the correlations of the dimensional analysis for heat transfer in solids and fluids,<sup>7,8</sup> on one hand, and, on the other, by finite element formulation of the Reynolds averaged Newton-Stokes (RANS) equations.<sup>9</sup> The numerical simulation has been performed with the FEM code COMSOL Multiphysics,<sup>®</sup> release 4.4.<sup>10</sup>

## 2. MICRO GAS TURBINE LAYOUT AND TE MODULES MAIN FEATURES

Figure 1 shows the layout of the micro gas turbine (MGT) and thermoelectric generator (TEG) coupled system. In the thermoelectric generator, the heat source is provided by exhaust gas and the heat sink is cooled by water. Hence, hot and cold sides of TEG are supplied by the cogeneration system for the production of hot water.

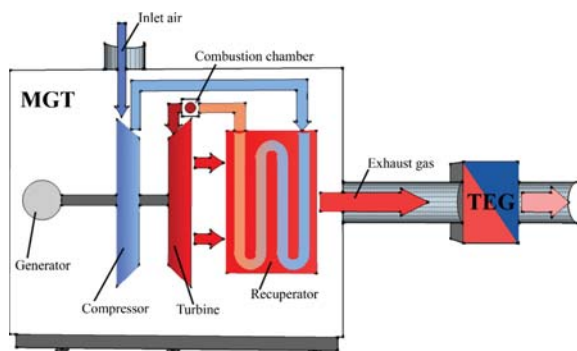


**Figure 1.** Layout of the micro gas turbine (MGT) and thermoelectric generator (TEG) coupled system. Main components of the MGT are indicated.

**Table I.** Turbec T100 P technical data.<sup>5</sup>

Electrical output:	100 kW
Electrical efficiency:	30 %
Fuel consumption:	333 kW
Exhaust gas flow:	0.80 kg/s
Exhaust gas temperature:	270 °C
Nominal volumetric exhaust gas emissions	
@ 15% O <sub>2</sub> , 100% load	
NO <sub>x</sub> :	<6 ppm/v
CO:	<6 ppm/v
Maximum volumetric exhaust gas emissions	
@ 15% O <sub>2</sub> , 100% load	
NO <sub>x</sub> :	<15 ppm/v
CO:	<15 ppm/v

### 2.1. MGT Layout

In this work, the micro gas turbine (MGT) Turbec T100P<sup>5,6</sup> has been considered. Its main components are a radial compressor, a tubular combustor, a recuperator, a radial turbine and the electrical generator (Fig. 1). Turbec T100P produces an electrical power of 100 kW with a global efficiency of 30%. Flue gas can be regarded as a mix of air, CO<sub>2</sub> and water vapor; the maximum content of NO<sub>x</sub> and CO is less than 15 ppm @ 15% O<sub>2</sub> (Table I). Exhaust gas temperature is 270 °C; mass flow is 0.80 kg/s; as exhaust pipe diameter is 30 mm, flue gas flow presents high Reynolds number ( $Re \approx 122000$ , fully developed turbulent flow). Exhaust gas properties at 270 °C can be taken as follows: density  $\rho_g = 0.64 \text{ kg/m}^3$ , specific heat  $c_p = 1.035 \text{ kJkg}^{-1}\text{K}^{-1}$ ; viscosity  $\mu_g = 2.8 \times 10^{-5} \text{ Pa}\cdot\text{s}$ , thermal conductivity  $k_g = 0.042 \text{ Wm}^{-1}\text{K}^{-1}$ .

### 2.2. TE Modules Characteristics

Commercial available thermoelectric modules operating in the 30 °C–200 °C temperature range are based on bismuth and antimony tellurides. In the considered temperature range, these thermoelectric materials present average ZT values varying between 0.6 and 0.9. Thus, the expected efficiency range of TEG modules is 3–6%. The features of typical commercial 40 mm × 40 mm TE modules for power generation are summarized in Table II.<sup>13–17</sup>

In the evaluation of the coupled system, a precautionary value of 4% for TEG modules efficiency has been considered. With this value, the thermal flux that has to be recovered from the exhaust gas is  $Q_{\min} = 12.5 \text{ kW}$ . The required number of TE modules varies between 52 and 104, depending on the output power in the range 0.28–0.59 W/cm<sup>2</sup>.

**Table II.** Main features of commercial 40 × 40 mm<sup>2</sup> TEG modules.

	P [W/cm <sup>2</sup> ]	$\eta$ [%]
$\Delta T = 100^\circ\text{C}$	0.10–0.22	3.2–3.6
$\Delta T = 170^\circ\text{C}$	0.28–0.59	4.6–5.4
$\Delta T = 200^\circ\text{C}$ (*)	>0.6	~6.0

Note: (\*) Operating with  $T_c = 20^\circ\text{C}$  and  $T_h = 220^\circ\text{C}$ .

### 3. SUITABLE CONFIGURATIONS FOR A MGT—TEG COUPLED SYSTEM

Three suitable arrangements for the integrated MGT—TEG system have been evaluated. In the first solution, TEG modules are located directly on the external surface of the exhaust pipe. In the other configurations, waste heat is transported from the exhaust pipe to an external thermoelectric generator, by using a compact heat exchanger and a suitable working fluid, or by means of heat pipes.

#### 3.1. Configuration with TEG Modules Located on the External Surface of the Exhaust Pipe

Figure 2 depicts the schematic of the coupled system with TE modules placed directly on the external surface of the exhaust pipe. The internal area of the pipe has to be enhanced by fins (Fig. 2) to increase the heat transfer. The evaluated geometry of the pipe segment allows the location of 10 ranks of thermoelectric modules. The heat transfer coefficient of flue gas  $h$  [ $\text{Wm}^{-2}\text{K}^{-1}$ ] has been evaluated using the correlations of the dimensional analysis for the calculation of the Nusselt number:

$$Nu_L = \frac{hL}{k}$$

where  $L$  [m] is a characteristic length of the flow,  $k$  [ $\text{Wm}^{-1}\text{K}^{-1}$ ] is the thermal conductivity of the fluid (exhaust gas). In the case of turbulent pipe flow, Nusselt number can be evaluated as a function of fluid flow characteristics, fluid properties and pipe roughness:

$$Nu_D = f\left(Re_D, Pr, \frac{e_s}{D}\right)$$

where  $D$  [m] is the pipe diameter,  $Re_D$  is the Reynolds number with  $D$  as characteristic length ( $Re_D = uD/\nu$ ,  $u$  velocity magnitude [m/s],  $\nu$  kinematic viscosity [ $\text{m}^2/\text{s}$ ]),  $Pr$  the Prandtl number ( $Pr = \nu/\alpha$ ,  $\alpha$  thermal diffusivity [ $\text{m}^2/\text{s}$ ]) and  $e_s$  [m] is the pipe roughness. The evaluation of the heat transfer coefficient with the expressions for smooth pipes (Dittus-Boelter, Petukhov),<sup>7</sup> yielded 27–32  $\text{Wm}^{-2}\text{K}^{-1}$  for the MGT exhaust pipe. Taking into account the pipe roughness, values up to

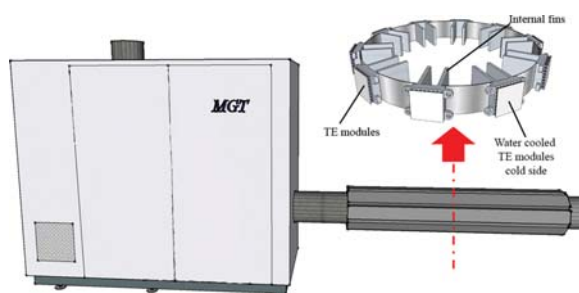


**Figure 2.** Schematic of the configuration with TE modules placed on exhaust pipe external surface. The inner surface of the pipe, in the waste heat recovery segment, is enhanced by fins.

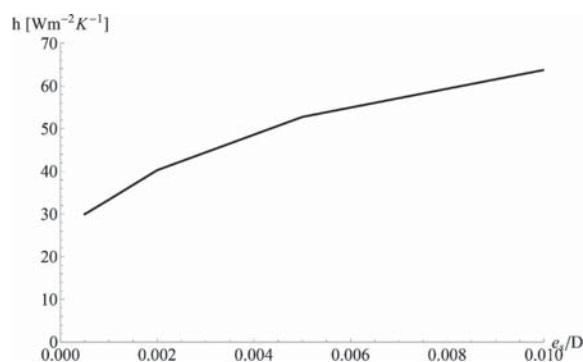


**Figure 3.** Heat transfer coefficient  $h$  [ $\text{Wm}^{-2}\text{K}^{-1}$ ] in exhaust gas as a function of pipe relative roughness  $e_s/D$ .

60  $\text{Wm}^{-2}\text{K}^{-1}$  have been obtained. Figure 3 shows heat transfer coefficient as a function of pipe relative roughness  $e_s/D$ .

In this configuration, the thermoelectric modules are directly integrated into a heat exchanger flue gas/water. The evaluation of the flue gas/water counterflow heat transfer with 0.2 l/s water mass flow rate (inlet temperature 30 °C), through a multi-layered 3 mm aluminium—5 mm TE modules ( $k_{\text{TEG}} = 1.42 \text{ Wm}^{-1}\text{K}^{-1}$ )—3 mm aluminium wall and with 100 mm wide fins, has led to a minimum pipe segment  $l_{\text{min}} \approx 90 \text{ cm}$  to achieve  $Q_{\text{min}} = 12.5 \text{ kW}$ . In Figure 4(a), mean temperature profiles in exhaust gas and water sides are reported. Figure 4(b) reports the temperature distribution in the exhaust gas evaluated with finite element analysis (FEA). FE analysis of heat transfer through a finned pipe segment shows high temperature gradient within the boundary layer. Hence, some difference between the straight line of the gas side temperature reported in Figure 4(a) and the temperature profile in the TE modules hot side has to be expected. The electrical arrangement of the modules could be made connecting in

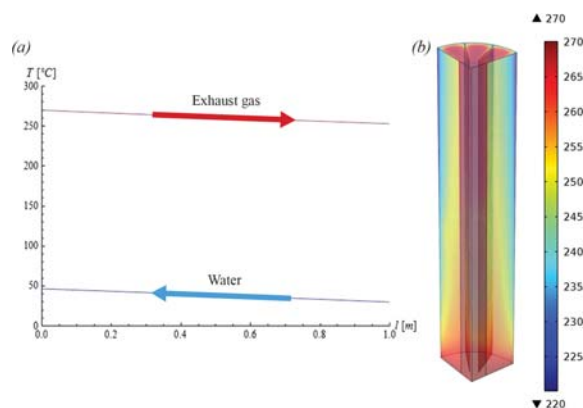


**Figure 4.** Counterflow exhaust gas–water heat exchanger. (a) Mean temperature profiles [°C] in exhaust gas (red) and water (blue). (b) Temperature distribution [°C] in an internally finned pipe: high temperature gradient occurs in the boundary layer near the wall pipe.

series the modules in each rank; the ranks then should be connected in parallel.

### 3.2. Configuration with Finned Pipe Heat Exchanger and TEG Located Outside the Exhaust Pipe

The second evaluated heat recovery configuration is based on the utilization of a compact heat exchanger, to transport heat from the flue gas to the TEG hot side by means of a working fluid. Figure 5 depicts a suitable layout of the integration of a finned pipe heat exchanger into the exhaust pipe. The exhaust gas flow through the pipe bundle yields higher values of heat transfer coefficient. Nusselt and Reynolds numbers must be referred to the diameter of the bundle tubes  $d$  as characteristic length and to the maximum velocity value. Figure 6 plots Nusselt number values across the tubes bundle, calculated by using the results of finite element (FE) fluid flow evaluation in the expression:<sup>8</sup>

$$Nu_d = Pr^{0.36} fn(Re_d)$$

where, for high Reynolds flow across aligned rows bundle, it can be considered:  $fn(Re_d) = 0.27Re_d$ . With a Nusselt number up to 150, exhaust gas flow across the tubes bank can achieve a heat transfer coefficient up to  $185 \text{ Wm}^{-2}\text{K}^{-1}$ . Heat transfer may be increased by fins. Flat thin fins, with thickness 1 mm and pitch 10 mm, have been considered across the bundle, as shown in Figure 7. Fins efficiency is the ratio of global fin heat transfer rate to the heat transfer rate of the fin entirely at the bundle tubes wall temperature.<sup>7,11</sup> Efficiency  $\eta_f$  can be calculated as:

$$\eta_f = \frac{Q}{Q_{id}} = \frac{\int_{A_f} h(T_f - T) dA}{h(T_f - T_w) A_f}$$

where  $A_f$  is the fins area [ $\text{m}^2$ ],  $h$  is the coefficient of heat transfer [ $\text{Wm}^{-2}\text{K}^{-1}$ ],  $T_f$  is the temperature of flue gas [K],

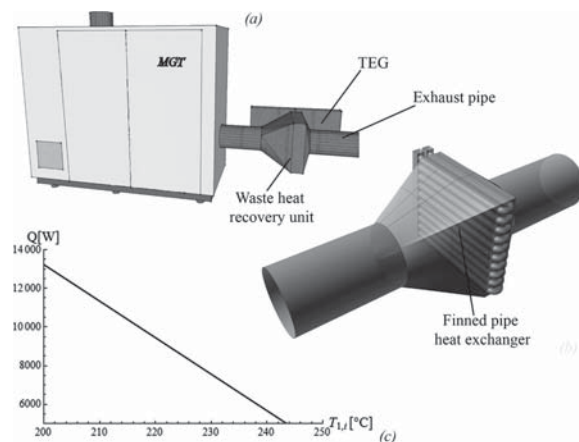


**Figure 5.** Suitable configuration of waste heat recovery from MGT exhaust gas by a finned pipes heat exchanger. (a) Layout of the coupled system in the considered configuration; (b) detail of the waste recovery unit; (c) heat flow [W], recovered by the finned pipes heat exchanger, as a function of the working fluid inlet temperature.

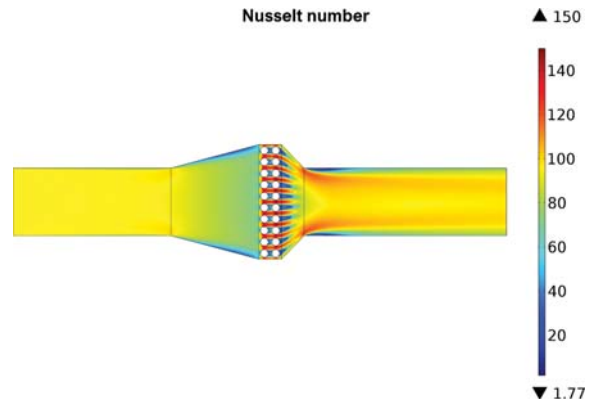


**Figure 6.** Nusselt number of flue gas flow across the pipe bundle. Maximum heat transfer coefficient was found  $h_{max} = 185 \text{ Wm}^{-2}\text{K}^{-1}$ .

$T$  is the local value of temperature on the fin [K],  $T_w$  is the wall temperature of the tubes [K]. Fins efficiency is, hence, calculated from the temperature distribution on the fins, plotted for the single fin in Figure 7. With the current geometry, fins efficiency was evaluated as  $\eta_f \approx 88\%$ . The considered configuration achieves high heat transfer area, up to  $3 \text{ m}^2$ , with a very small heat exchanger volume ( $\sim 30 \text{ l}$ ). In the evaluation of the waste heat recovery unit, a synthetic fluid with the following properties at  $200 \text{ }^\circ\text{C}$  was considered:<sup>18</sup> density  $\rho_f = 900 \text{ kg/m}^3$ ; specific heat  $c_p = 2.2 \text{ kJkg}^{-1}\text{K}^{-1}$ , thermal conductivity  $k_f = 0.1 \text{ Wm}^{-1}\text{K}^{-1}$ , viscosity  $\mu_f = 0.5 \text{ mPa} \cdot \text{s}$ . The recovered heat flow as a function of the working fluid inlet temperature, with a fluid mass flow rate of  $1 \text{ l/s}$ , is shown in Figure 5. With a fluid inlet temperature of  $204 \text{ }^\circ\text{C}$ , recovered heat has been evaluated as  $Q = 12.5 \text{ kW}$ . Pressure drop in flue gas across the pipes bank was evaluated with FE analysis. Figure 8 shows a slice plot of pressure drop across the waste heat recovery unit: maximum

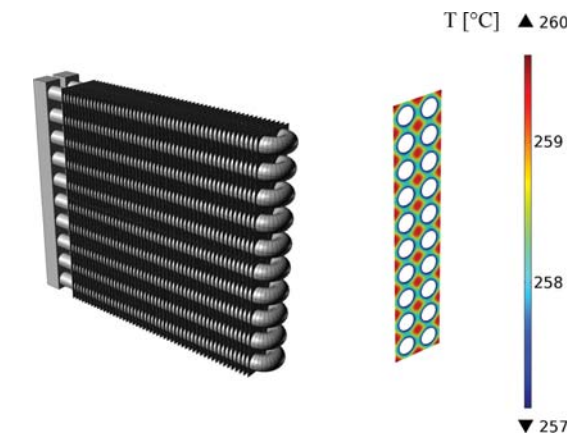


**Figure 7.** Compact heat exchanger flat fins: the efficiency is evaluated from the temperature distribution on the fins. Plot of temperature distribution on the single fin [°C]

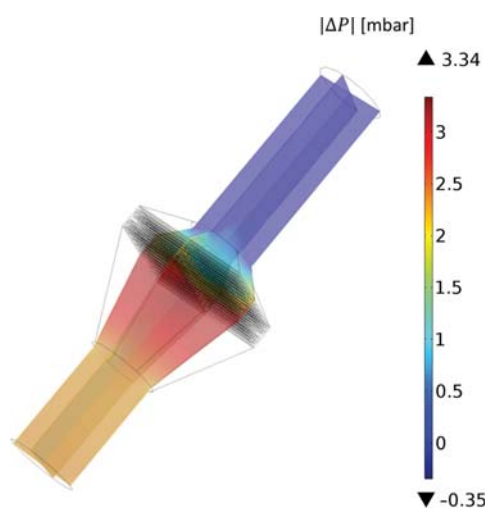


**Figure 8.** Pressure drop in the waste heat recovery unit (finned pipes heat exchanger).

calculated pressure drop is  $\Delta P_{\max} \approx 3.4$  mbar corresponding to a minimum efficiency drop,<sup>5</sup> which can be easily recovered with the proposed thermoelectric generator. In this configuration, recovered heat is transported to the thermoelectric generator, outside the exhaust pipe. Heat flux on the hot side of the thermoelectric generator is provided by the working fluid used in the finned heat exchanger to recover waste heat from the exhaust gas. Temperature increase of water (TEG cold side) and cooling of working fluid (hot side) depend on the ratio of mass flow rates. Thus, in this configuration, hot side temperature can be adjusted by setting working fluid mass flow rate properly, whereas, with the previous solution, hot side temperature was definitively determined by the fixed mass flow rate of the exhaust gas. On the thermoelectric generator, modules can be arranged in 5 banks of 100 W each; in this configuration, the modules in each bank should be connected in series, whereas banks should be connected in parallel.

### 3.3. Configuration with Waste Heat Recovery by Means of Heat Pipes

The last considered solution for waste heat recovery is heat transportation from the exhaust pipe to the thermoelectric generation using heat pipes. Figure 9 plots the layout of a heat pipe:<sup>12</sup> the heat is transported from the hot side (evaporator), where the working fluid vaporizes, through an adiabatic segment, to the cold side (condenser), where the vapor is condensed. The liquid mass flow rate is pumped back to the evaporator by capillary forces through the perimeter wicking structure. A suitable schematic of the configuration of waste heat recovery by means of heat pipes is shown in Figure 10. In this work, horizontal heat pipes with an external diameter (sealed container) of 16 mm and effective length of 15 cm (total length 22.5 cm) have been considered. Heat pipe effective length

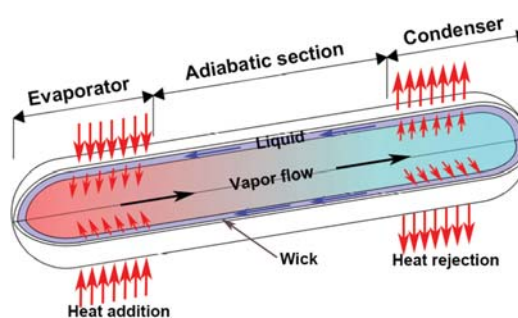


**Figure 9.** Schematic of a heat pipe.

is defined as  $l_{\text{eff}} = 0.5l_e + l_a + 0.5l_c$ , where  $l_e$ ,  $l_a$ ,  $l_c$  are evaporator, adiabatic and condenser regions lengths. For 250 °C–270 °C temperature range, Dowtherm A<sup>®</sup> has been considered as working fluid. Saturated liquid properties at 257.1 °C (atmospheric boiling temperature) are reported in Table III.

Surface tension has been taken as  $\sigma_l = 0.014$  N/m. The number of merit [ $\text{W}/\text{m}^2$ ] of a heat pipe working fluid is defined as:

$$M = \frac{\rho_l \sigma_l L}{\mu_l}$$

For the considered operating fluid,  $M = 1.31 \times 10^{10}$   $\text{W}/\text{m}^2$ . The number of merit has been used to evaluate the maximum heat flow rate recovered by a single heat pipe with reference to the *wicking limit*. The evaluation of the other operating limitations (*viscous*, *sonic*, *entrainment*, *boiling limits*)<sup>11,12</sup> yielded higher heat transfer rates, with values from 1.2 kW (entrainment limit) up to 66 kW (sonic limit). The wicking limit is linked to the maximum liquid mass flow rate that capillary forces can pump back to the evaporator. Maximum capillary pumping pressure must be greater than the sum of the pressure drops in the liquid

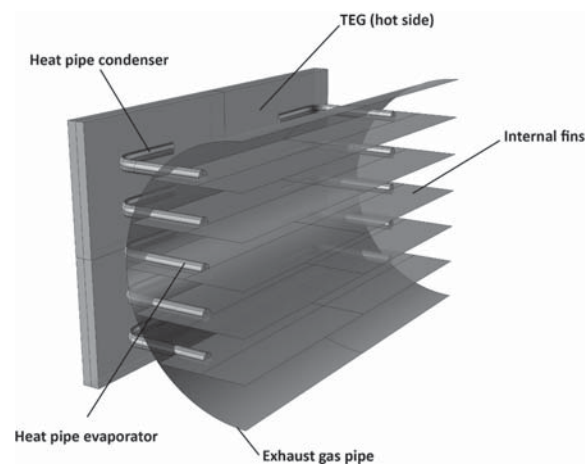


**Figure 10.** Schematic of the configuration of waste heat recovery from exhaust gas using heat pipes.

**Table III.** Saturated liquid properties at 257.1 °C of the considered working fluid for the heat pipes.<sup>18</sup>

Density	$\rho_l = 851.9 \text{ kg/m}^3$
Specific heat:	$c_{pl} = 2.237 \text{ kJkg}^{-1}\text{K}^{-1}$
Thermal conductivity:	$k_l = 0.101 \text{ Wm}^{-1}\text{K}^{-1}$
Viscosity:	$\mu_l = 0.27 \text{ mPa}\cdot\text{s}$
Vaporization latent heat:	$L = 296.4 \text{ kJ/kg}$

(flow from the condenser back to the evaporator) and in the vapor (flow from the evaporator to the condenser) plus the hydrostatic pressure drop, depending on the inclination  $\varphi$  of the pipe:

$$\Delta P_{c,\max} \geq \Delta P_l + \Delta P_v + \Delta P_g$$

If liquid properties and wicking structure do not vary along the pipe, the maximum liquid mass flow rate satisfying the above condition is:

$$\dot{m}_{\max} = \left[ \frac{\rho_l \sigma_l}{\mu_l} \right] \left[ \frac{KA_w}{l_{\text{eff}}} \right] \left[ \frac{2}{r_e} - \frac{\rho_l g l_{\text{eff}}}{\sigma_l} \sin \varphi \right]$$

where  $K$  is the wick permeability [ $\text{m}^2$ ],  $A_w$  is the wick cross-sectional area [ $\text{m}^2$ ],  $r_e$  the effective capillary radius [ $\text{m}$ ]. The corresponding maximum heat flow  $Q_{\max}$  [ $\text{W}$ ] is:

$$Q_{\max} = \dot{m}_{\max} L = M \left[ \frac{kA_w}{l_{\text{eff}}} \right] \left[ \frac{2}{r_e} - \frac{\rho_l g l_{\text{eff}}}{\sigma_l} \sin \varphi \right]$$

The wick has been considered as follows:<sup>12</sup> permeability  $K = 1.6 \times 10^{-10} \text{ m}^2$ , 80% porosity, thickness  $t_w = 3 \text{ mm}$ , pore radius 0.0015 cm. The chosen geometry of the pipe, with  $\varphi = 0$  (horizontal pipe), led to a maximum mass flow rate 0.7 g/s. Thus, maximum heat transport, for the single heat pipe, has been found  $Q_{\max} = 207 \text{ W}$ . This means that at least 12 heat pipes for 100 W produced electrical power are required. To produce 500 W electrical power with this waste heat recovery configuration, the thermoelectric generator should be splitted into 5 banks connected in parallel, as for the solution with the compact heat exchanger; the TE modules in each bank would be connected in series.

#### 4. CONCLUSIONS

The feasibility of a coupled micro gas turbine (MGT) and thermoelectric generator (TEG) system has been evaluated. The aim was to increase the production of electrical power, by generating a minimum power of 500 W with the TE device. In the evaluated configurations, the thermoelectric generator is thought as integrated into a cogeneration system for the production of electrical power and hot water. Three different strategies for waste heat recovery from MGT exhaust gas have been considered. In the first one, the TE modules are placed directly on the external surface of the exhaust pipe. In this configuration no fluid pumping is required and negligible efficiency drop for the microturbine, due to pressure drop in the exhaust gas across

the TEG section, is to be expected. In the second configuration, with waste heat recovery from the exhaust gas through a finned heat exchanger, the thermoelectric generator is located outside the exhaust pipe. This solution leads to a compact waste heat recovery unit and to easier control of TEG hot and cold sides temperature, by setting mass flow rates of heat exchanger working fluid and water properly. On the other hand, in comparison with the previous presented solution, a circulator pump for the working fluid is required. Furthermore, pressure drop in the exhaust gas across occurs. The pressure drop must be minimized, to avoid efficiency drop in microturbine and, hence, in the whole integrated system. The third presented solution is based on the use of heat pipes for waste heat recovery from exhaust gas and transport of thermal energy to the thermoelectric generator hot side. This configuration may require a high number of them for the production of the needed electrical power ( $\sim 12$  every 100 W generated electric power). Furthermore, heat pipes length has to be limited as much as possible, in order to preserve their heat transfer features. Nonetheless, the use of heat pipes enhances adaptability to a large output power range. This solution does not require any fluid pumping, as the first one presented in this work. Integrating the thermoelectric generator into a cogeneration system was considered to be the only feasible solution for the MGT—TEG arrangement. The cogeneration system supplies heat source and heat sink for the thermoelectric generator, therefore the cost of the coupled system is reduced to that of TE modules. Furthermore, by increasing electrical output power the integration of the TEG into a cogeneration system allows to balance potential microturbine efficiency drops due to the insertion of a heat exchanger for hot water production.

**Acknowledgments:** This work has been funded by the Italian National Research Council—Italian Ministry of Economic Development Agreement “Ricerca di sistema elettrico nazionale.”

#### References and Notes

1. G. J. Snyder, *Energy Harvesting Technology*, edited by S. Priya and D. J. Inman, Springer, New York (2009), p. 325.
2. D. M. Rowe, *Thermoelectrics Handbook Macro to Nano*, edited by D. M. Rowe, CRC Press, Boca Raton (2005), p. 1.
3. T. Hendricks and T. Choate, *Engineering Scoping Study of Thermoelectric Generator Systems for Industrial Waste Heat Recovery*, (Industrial Technologies Program) U.S. Department of Energy, (2006)
4. S. LeBlanc, *Sustainable Mater. Technol.* 1–2, 25 (2014)
5. Turbec (Ansaldo), *Technical Description—T100 Natural Gas* (2012).
6. R. Calabria, P. Massoli, F. Chiariello, and F. Reale, *Proceedings of ASME Turbo Expo*, Montreal (2015).
7. W. M. Rohsenow, J. P. Hartnett, and Y. I. Cho, *Handbook of Heat Transfer*, 3rd edn., McGraw-Hill, New York (1998).
8. J. H. Lienhard IV and J. H. Lienhard V, *A Heat Transfer Textbook*, 3rd edn., Phlogiston Press, Cambridge (MA) (2008).

9. O. C. Zienkiewicz, R. L. Taylor, and P. Nithiarasu, *The Finite Element Method for Fluid Dynamics*, Butterworth-Heinemann, Oxford (2005).
10. COMSOL Multiphysics Documentation, Release 4.4 (2013).
11. R. K. Shah and D. P. Sekulić, *Fundamentals of Heat Exchanger Design*, Wiley & Sons, Hoboken, NJ (2003).
12. D. Reay and P. Kew, *Heat Pipes*, Butterworth-Heinemann, Oxford, UK (2006).
13. FERROTEC NORD Corp., <http://www.ferrotec-nord.com/>.
14. European Thermodynamics Ltd., <http://www.europanthermodynamics.com/>.
15. KRYOTHERM, <http://www.kryothermtec.com/>.
16. THERMALFORCE, <http://www.thermalforce.de/>.
17. TEGPro, <http://www.tegpro.com/>.
18. Dow Heat Transfer Fluids, <http://www.dow.com/heattrans/products/synthetic/dowtherm.htm>.

Received: 1 April 2016. Accepted: 25 May 2016.